JOURNAL OF VIROLOGY, Dec. 1993, p. 7106–7117
0022-538X/93/127106-12$02.00/0

Vol. 67, No. 12

5′ Sequences of Rubella Virus RNA Stimulate Translation of Chimeric RNAs and Specifically Interact with Two Host-Encoded Proteins

GREGORY P. POGUE, XI-QING CAO,† NISHI K. SINGH, AND HIRA L. NAKHASI*

Laboratory of Molecular Pharmacology, Division of Hematologic Products, Center for Biologics Evaluation and Research/Office of Therapeutic Research and Review, Food and Drug Administration, Bethesda, Maryland 20892

Received 19 July 1993/Accepted 8 September 1993

Sequences at the 5′ and 3′ ends of the rubella virus (RV) genomic RNA can potentially form stable stem-loop (SL) structures that are postulated to be involved in virus replication. We have analyzed the function of these putative SL structures in RNA translation by constructing chimeric chloramphenicol acetyltransferase (CAT) RNAs, flanked either by both 5′- and 3′-terminal sequence domains from the RV genome or several deletion derivatives of the same sequences. After in vitro transcription of chimeric RNAs, the translational efficiencies of these RNAs were compared by the rabbit reticulocyte lysate translation system. For in vivo translation studies, the level of CAT activity was measured for chimeric RV/CAT RNAs expressed in transfected cells by the adenovirus major late promoter. Both in vivo and in vitro translation activities of the chimeric RNAs revealed that the presence of 5′ and 3′ SL sequences of RV RNA, in correct (+) orientation and context [5′(+)SL and 3′(+)SL, respectively] was necessary for efficient translation of chimeric RV/CAT RNAs. The presence of the RV 5′(+)SL sequence had the primary enhancing effect on translation. To identify host proteins which interact with the 5′(+)SL which may be involved in RV RNA translation, RNA gel-shift and UV cross-linking assays were employed. Two host proteins 59 and 52 kDa in size, present in cytosolic extracts from both uninfected and RV-infected cells, specifically interacted with the RV 5′(+)SL RNA. Direct binding comparisons between wild-type and mutant 5′(+)SL RNAs demonstrated that sequences in and around the bulge region of the terminal stem domain of this structure constituted a protein binding determinant. Human serum, qualified for anti-Ro/SS-A antigen specificity, immunoprecipitated 59- and 52-kDa protein-RNA complexes containing the RV 5′(+)SL RNA. However, poly- and monoclonal antisera raised against the recombinant 60- and 52-kDa Ro proteins failed to precipitate complexes containing the 5′(+)SL RNA. The identity of the proteins binding this RV *cis*-acting element remains to be determined; however, their role in RV translation is discussed.

Rubella virus (RV), the causative agent of German measles, is a positive-strand RNA virus composed of a single genomic RNA (9,757 nucleotides [nt]) beginning with a 5′ 7-methyl guanosine cap structure and 3′ poly(A) tract (6, 31). The RV genome contains two long open reading frames (ORFs), a 5′ proximal ORF that encodes the nonstructural proteins (6) and a 3′ proximal ORF that encodes the three virus structural proteins (25, 30, 31, 41). In RV-infected cells, a subgenomic RNA is synthesized from which the 3′ proximal ORF is expressed (31).

Comparison of RV genomic sequences with those of the *Alphaviruses* does not reveal significant overall homology; however, some sequence elements conserved among the *Alphaviruses* are also found within the RV genome (6). A short (41-nt) 5′ nontranslated region (NTR) precedes the initiation codon for nonstructural protein synthesis, which is contained within a putative stem-loop (SL) structure ($\Delta G = -19$ kcal/mol [see Fig. 5]) (6) and is structurally conserved between RV and Sindbis virus genomes. Primer extension analysis of the 5′ end of the RV genomic RNA revealed strong signals corresponding to the position of this predicted SL structure, strongly suggesting its existence in solution (6). The 3′-terminal region of the RV genome also contains a stable SL structure which is bound specifically by three host-encoded proteins present in Vero 76 cytosolic extracts (26). These interactions depend on the phosphorylation status of such proteins (26), and the identity of one protein has now been established (27) as calreticulin (18, 38).

SL structures have been implicated in the processes of RNA virus translation, RNA replication, and encapsidation (1, 8, 11, 19, 20, 21, 24, 26, 32, 35, 39). Recently, we have shown that the presence of both the 5′ and 3′ SL sequences of RV RNA in the correct orientation [5′(+)SL and 3′(+)SL, respectively] is necessary for the initiation of negative-strand synthesis from chimeric chloramphenicol acetyltransferase (CAT) template in RV-infected cells (27). Indeed, binding determinants of several cellular and virus-encoded RNA binding proteins have been demonstrated to be contained within SL structures (1, 3, 5, 13, 20, 21, 23, 24, 26, 32). Many recent studies have sought to define sequence and structural domains responsible for promoting translation of RNA virus genomes. The majority of these efforts have focused on defining sequence elements that facilitate cap-independent translation of picornavirus genomes. Translation of genomic RNA from this group of viruses, which includes poliovirus and encephalomyocarditis virus, is dependent on an extended domain within the 5′ NTR sequence termed the internal ribosomal entry site or ribosomal landing pad (8, 12, 28, 33, 34). Within this domain of highly complex secondary structure, several structural features, a polypyrimidine tract flanked by two extended SL structures, profoundly influence translation of poliovirus proteins (11). The SL structure present immediately 5′ of the polypyrimidine tract must be preserved for both poliovirus translation and

* Corresponding author.

† Present address: Laboratory of Pulmonary and Molecular Immunology, National Heart, Lung, and Blood Institute, Bethesda, MD 20892.

infectivity (11). Recently, it has been shown that a host-encoded protein, the La antigen, which binds to an SL structure in the poliovirus 5′ NTR can stimulate and correct aberrant translation in rabbit reticulocyte lysate (21).

We are interested in determining sequences within the RV genome which promote translation from RV-encoded initiation codons and identifying cellular proteins which may be involved in this process. In the absence of an RV cDNA clone from which infectious RNA can be derived, we have constructed chimeric reporter RNAs composed of the CAT gene flanked by the RV 5′- and 3′-terminal sequence domains, which contain putative SL structures. These constructs, including several mutant derivatives, were tested for their ability to promote translation both in vitro and in vivo. Synthetic RNAs corresponding to specific sequence elements within the RV genome were used to study RNA-protein interactions.

In the present study, we demonstrate that the 5′- and 3′-terminal sequence elements from RV RNA promote the translation of chimeric CAT RNAs in vitro and in vivo. An SL structure, containing the authentic RV initiation codon, within the RV 5′ *cis*-acting element is specifically bound by two host-encoded proteins which show specificity for autoimmune sera.

MATERIALS AND METHODS

Virus infection of cells. Vero 76 cells were grown in Dulbecco's modified Eagle's medium supplemented with 10% fetal calf serum (Hyclone Inc.). Cells were infected with plaque-purified M33 strain of RV (5 PFU/cell) as previously described (26).

Preparation of cell lysates. Cell lysates from both uninfected and infected cells were prepared as described previously (26) in a cytolysis buffer (25 mM Tris-HCl buffer [pH 7.5] containing 40 mM KCl, 1% Triton X-100, 25 μM *p*-nitrophenyl *p*′-guanidino-benzoate, and 10 μg of leupeptin per ml). Protein concentration was determined by the bicinchoninic acid assay (Pierce).

In vitro synthesis of RNA transcripts. Synthesis and purification of oligonucleotide templates that include a 17-base T7 promoter were performed as previously described (22, 26). Transcription reactions with T7 polymerase were performed with the T7 Megascript Kit (Ambion, Inc.) according to the manufacturer's protocol. The reverse-complement sequences of the putative structures presented in Fig. 5 comprise the oligonucleotide sequence used for the synthesis of the wild-type RV 5′(+)SL RNA and derivative mutants. For example, the oligonucleotide sequence for the wild-type 5′(+)RV (with the complementary sequence of the T7 promoter underlined) is: 5′ACCTCATCTAGGAGTTTCTCCATGGGAATGGGA GTCCTAAGCGAGGTCCTATA [GTGAGTCGTATTA 5′ (+)SL]. pT7hY3RNA plasmid DNA (the kind gift of Sandra Wolin, Yale University) was linearized with *Dra*I, and runoff T7 RNA transcripts were synthesized in vitro with the T7 Megascript Kit.

RNA gel-retardation assays. RNA gel-shift assays were conducted by incubating 0.3 ng (20,000 cpm) of a high-specific-activity (70,000 cpm/ng) RNA probe with 20 μg of cytoplasmic lysates from mock- or RV-infected cells in cytolysis buffer containing 2 U of Inhibit-ACE (5′-3′ Inc.). Reaction mixtures were incubated at room temperature for 30 min and resolved for 1.5 h in 6% polyacrylamide gel (Protogel; National Diagnostics) buffered in Tris-borate-EDTA buffer (0.089 M Tris-HCl [pH 8.3] containing 0.089 M boric acid and 0.002 M EDTA). After electrophoresis, gels were dried and RNA-protein complexes were visualized by subsequent autoradiography.

In vitro UV-induced cross-linking and SDS-PAGE analysis of cross-linked proteins. Cell lysates (28 μg of protein) from uninfected or infected cells were incubated with 0.7 ng (~3.55 nM) of high-specific-activity RNA probe (70,000 cpm/ng) for 30 min at either 0°C or room temperature. RNA-protein complexes were cross-linked at 0°C with a UV Stratalinker 2400 (Stratagene Inc.) for 30 min at 1,200 μJ × 100. Samples were treated with 1 U of RNase T_1 (GIBCO/BRL) for 10 min at room temperature. This step was not included in all assays because RNA-protein complexes of the same molecular mass were obtained in assays with or without RNase T_1 treatment (36). Samples were boiled in Laemmli sample buffer and analyzed by sodium dodecyl sulfate-polyacrylamide gel electrophoresis (SDS-PAGE [10% polyacrylamide]) (Protogel; National Diagnostics) and autoradiography.

Immunoprecipitation of protein-RNA complexes. Various antisera were employed in immunoprecipitation reactions, including (i) human polyclonal serum (Ge) derived from patients suffering from autoimmune disorders with antibodies to both the 60- and the 52-kDa Ro/SS-A proteins (2, 2a), (ii) mouse monoclonal antiserum (A6) raised against recombinant 60-kDa Ro/SS-A protein (kind gift of E. K. L. Chan), (iii) rabbit polyclonal antiserum raised against recombinant 60-kDa Ro/SS-A protein (kind gift of Jack Keen), (iv) rabbit polyclonal serum (no. 6739) raised against recombinant 52-kDa Ro/SS-A protein (kind gift of E. K. L. Chan), and (v) rabbit polyclonal antiserum raised against N- and C-terminal peptides of human calreticulin (kind gift of R. D. Sontheimer). After exposure of cell lysates (60 μg) containing 10^6 cpm of RV 5′(+)SL RNA or hY3RNA to UV light, appropriate volumes of antiserum were added to reaction mixtures and incubated at 4°C overnight with gentle rocking. A suspension of heat-killed, formalin-fixed *Staphylococcus aureus* cells (Immunoprecipitin; Bethesda Research Laboratories) was added to immunoprecipitation reaction mixtures to a final concentration of 5%. After a 3-h incubation at 4°C, material adhering to *S. aureus* cells was subjected to extensive washings with standard NET buffer (50 mM Tris [pH 8.0], 400 mM NaCl, 5 mM EDTA, 1% Triton X-100). Products from these reaction mixtures were analyzed by SDS-PAGE (10% polyacrylamide). Quantitation of resulting autoradiographs was performed with an LKB 2222-020 laser densitometer and a Molecular Dynamics personal laser densitometer.

Construction of plasmids. *Bam*HI-digested CAT insert derived from the pCM4 vector (Pharmacia), which contains the 5′ and 3′ noncoding sequence along with the entire CAT coding sequence, was isolated, and the ends were filled in with Klenow enzyme. This fragment was then blunt-end ligated into the filled-in *Spe*I site of the enhanced pADMLP vector (pD5; kindly provided by George Mark, Merck Sharp & Dohme Research Laboratories, Rahway, N.J.), which has an adenovirus major late promoter and simian virus 40 polyadenylation site. This construct was designated pPDCAT. The pPDCAT plasmid was digested with *Cla*I and *Nde*I restriction enzymes, filled in at both ends, and blunt-end ligated with the filled-in ends of a 165-bp *Nar*I-*Eco*RI fragment of the RV RVVC4 cDNA clone (41) and designated pPDCATSL4. The 165 nt of the RV 3′ terminus includes the 3′ SL structure and a 27-base poly(A) tail. The pPDCATSL4 plasmid was partially digested with *Bam*HI. The linearized plasmid was ligated with *Bam*HI-digested double-stranded oligonucleotide adapter, which contains the 65 5′ nt of the RV genomic RNA, and was designated pPDCATSL1. The plasmid with the 5′(+)SL sequence in the reverse orientation was designated pPDCATSL2. A double-

stranded oligonucleotide adapter without the sequences of loop m1 (see Fig. 5) of the 5′(+)SL structure (6) was ligated to pPDCATSL4 plasmid and designated pPDCATSL3. A single nucleotide deletion adjacent to AUG (nt 57) brought this codon in frame with the CAT ORF. The pPDCATSL5 plasmid was derived by digesting the pPDCATSL1 plasmid with *Nhe*I, which removes 105 nt from the 3′ end of RV RNA sequences. This modification deletes the 3′ SL structure but leaves the poly(A) tail region intact. pPDCATSL6 has a single nucleotide deletion in the RV 5′ NTR adjacent to AUG (nt 57), placing it in the same reading frame as the CAT AUG and shifting the RV AUG (nt 41) out of frame. The nucleotide sequences of all of the constructs were determined to verify the orientation of chimeric DNAs and the sequence at the junction regions.

Subcloning of PD5-derived plasmids in the pPGEM7Zf(+) vector. Oligonucleotide primers with restriction enzyme sites *Kpn*I and *Xba*I at the 5′ and the 3′ ends, respectively, were used to amplify the CATSL sequences from pPDCATSL plasmids. Amplified polymerase chain reaction DNA was digested with *Kpn*I and *Xba*I and ligated with pPGEM7Zf(+) vector (Promega). The nucleotide sequences of the constructs were determined to verify the orientation of chimeric DNAs and the sequence at the junction regions.

In vitro transcription and translation. 5′ capped RNA transcripts were synthesized in vitro from linearized plasmid pGEM-PDCAT and derivative vectors with SP6 RNA polymerase according to the SP6 Megascript Kit technical manual (Ambion, Inc.). RNA was quantitated by optical density and analyzed after agarose gel electrophoresis. Equal amounts of RNA (0.5 μg) from each sample were translated in vitro in rabbit reticulocyte lysates in the presence of [^{35}S]methionine. Total translation products were analyzed by SDS-PAGE (12% polyacrylamide) and subsequent fluorography (26).

Transfection of plasmid DNA and measurement of CAT activity. Subconfluent monolayers of Vero 76 cells in 60-mm tissue culture plates (about 10^6 cells) were used for transfection. Cells were washed twice with cold phosphate-buffered saline, and fresh Dulbecco's modified Eagle's medium was added. Plasmid DNA (10 μg) was diluted with 50 μl of sterile water and gently mixed with 50 μg (1 μg/μl) of lipofectin (GIBCO/BRL) per μl. The transfection mixture was incubated at room temperature for 10 min in a polystyrene tube and slowly dropped onto cells by gentle swirling of the plate. Cells were incubated at 37°C for different time periods after DNA transfection. Cells were harvested and CAT activity was measured as described in the Stratagene technical manual. The amount of radioactivity in nonacetylated and acetylated forms of chloramphenicol was quantitated with a Betascope 603 blot analyzer. Other quantitation was performed with an LKB 2222-020 laser densitometer.

RNA isolation and Northern blot analysis. Total RNA was isolated from cells at different times after transfection (25). Northern (RNA) blot analysis was done as previously described (7, 35).

RESULTS

Role of RV 5′- and 3′-terminal sequences in the translation of chimeric RV/CAT RNAs in vitro. To assess the translational role of the RV-terminal sequences, chimeric reporter constructs containing the CAT ORF flanked by the RV 5′- and 3′-terminal sequences were made. The resulting plasmid, denoted pPDCATSL1 (Fig. 1), contained the 5′ RV-terminal sequence (65 bp), which includes the 5′(+)SL (sense strand of RV virion RNA) and the 3′-terminal 165 nt of the RV genome, including the virus-encoded poly(A) sequence. This construct allowed in vitro transcription of RNA (PDCATSL1) with SP6 RNA polymerase. It should be noted that the authentic RV AUG initiation codon (nt 41 [Fig. 5]) (6) is in the same translational frame as the CAT reading frame. Two additional AUG codons (nt 3 and 57 [Fig. 5]) (6), contained within the 5′(+)SL, are normally not in frame with the RV-encoded nonstructural proteins (6). Translational initiation from the RV-encoded AUG (nt 41) of PDCATSL1 RNA should result in a chimeric RV/CAT protein ~29 kDa in size containing an additional 9 amino acids from RV nsP1 and 11 amino acids derived from the CAT 5′ NTR. Various mutations were introduced into the 5′ and 3′ SL regions of the pPDCATSL1 construct to ascertain which sequence domains are important in directing translation (Fig. 1). Schematic diagrams of each construct are shown in Fig. 1.

In order to determine nonsaturating concentrations of transcripts, various amounts of RNA transcripts from these constructs were tested for translational efficiency in the rabbit reticulocyte lysate translation system. On the basis of these results, translational comparisons were carried out with 0.5 μg of the RNA transcripts, whose integrity was confirmed by agarose gel electrophoresis. Products were labeled with [^{35}S]methionine. Qualitative differences in protein species synthesized from each RNA as well as relative quantitative differences in product levels could be determined by these in vitro assays.

PDCAT RNA, which lacks both RV flanking sequences and a poly(A) tail, did not function efficiently as a template for translation (Fig. 2, lane 2; Table 1). Addition of the 3′ 165 bp of RV RNA, which includes both the 3′(+)SL structure (sense strand of RV virion RNA) and RV-encoded poly(A) tail, to the CAT ORF (PDCATSL4 RNA) enhanced the synthesis of a 27-kDa CAT protein by 37-fold (Fig. 2, lane 6; Table 1). When both 5′ and 3′ RV sequences flanked the CAT ORF (PDCATSL1 RNA), two protein products were synthesized, one initiated from the CAT AUG codon (27 kDa) and a chimeric protein (RV/CAT hybrid) of higher molecular mass (29 kDa [Fig. 2, lanes 3 and 9]). Both protein products could be immunoprecipitated with antibodies raised against the CAT protein sequence (36). The RV/CAT chimeric protein (29 kDa) was the predominant protein product synthesized from PDCATSL1 RNA. Initiation from the CAT AUG of PDCATSL1 RNA (27-kDa CAT protein) was reduced by over 67% compared with that from PDCATSL4 RNA (Table 1). When the orientation of the 5′ RV leader sequence was reversed (PDCATSL2 RNA), leaving the CAT-encoded initiation codon and 3′ RV sequence unaltered, virtually no incorporation of radioactivity was observed (Fig. 2, lane 4), indicating that this inverted configuration of the 5′ SL structure strongly inhibited translation. A high level of the CAT protein product was synthesized in the reticulocyte lysate system from PDCATSL3 RNA, which contains a deletion in the RV 5′ leader sequence (nt 32 through 46) including the authentic RV-encoded AUG (Fig. 2, lane 5). A second protein, of slightly higher molecular mass (~28 kDa), was also synthesized from this RNA (Fig. 2, lane 5). This protein was probably initiated from an RV-encoded AUG codon at nt 57, placed in the same reading frame as the CAT initiation codon by a second deletion of single nucleotide directly adjacent to AUG (nt 57). This protein would be predicted to contain 4 RV-encoded amino acids and the 11 amino acids encoded by the CAT 5′ NTR in addition to the CAT protein. The 65% lower amount of RV/CAT chimeric protein produced from PDCATSL3 RNA, compared with that synthesized from PDCATSL1 RNA, shows the importance of sequence context on

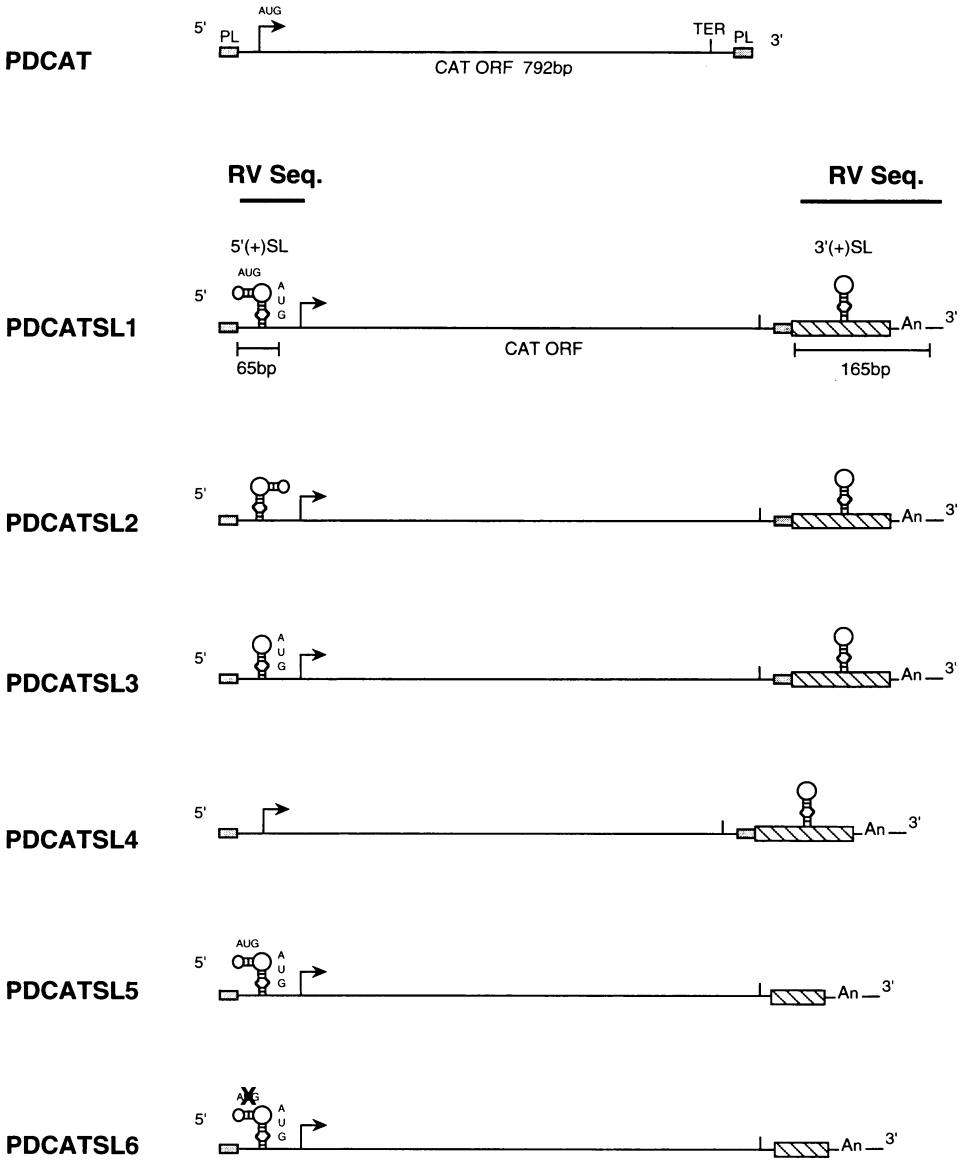

FIG. 1. Schematic representation of RV/CAT chimeric constructs. PDCAT consists of CAT coding region and its own 5′ and 3′ noncoding sequences. PDCATSL1 consists of CAT sequences plus both the initial 5′ 65 bases and the 3′-terminal 165 bases of RV genomic RNA. PDCATSL2 is the same as PDCATSL1, except the initial 5′ 65 bases are in a reverse orientation. PDCATSL3 has nucleotides 32 through 46 deleted from the 5′ 65 bases and AUG (nt 57) has been placed in the CAT reading frame by a single nucleotide deletion. PDCATSL4 has no 5′ 65 bases of RV genomic RNA. PDCATSL5 has 105 bases deleted from the 3′ 165 bases of RV RNA, which includes the 3′(+)SL sequences. PDCATSL6, which contains a 3′-terminal region identical to that of PDCATSL5, possesses a single base deletion in the 5′ RV sequences, placing the AUG (nt 41) out of frame and the AUG (nt 57) in frame with the CAT ORF. All of these constructs were either cloned into the enhanced pADMLP vector (PD5) or pGEM7Zf(+) vector. Arrows indicate the AUG codon in the CAT coding sequence. The relationship between the two RV-encoded AUGs and that present in the CAT coding region is shown in PDCATSL1. TER represents the termination codon, while PL indicates a few 5′ and 3′ nucleotides derived from vector-encoded polylinker sequences. Seq., sequence.

the initiation of translation from the authentic RV-encoded AUG codons (Table 1).

PDCATSL5 RNA has an unaltered 5′ RV leader sequence and poly(A) tail, but the 3′(+)SL sequence (nt 9669 to 9700 of the RV genomic RNA [6]) and immediate flanking bases have been deleted. A similar profile of protein products, compared with PDCATSL1 RNA, was synthesized from PDCATSL5 RNA with the overall level of translation reduced by ~50% (Fig. 2, lane 10; Table 1). This result, taken together with the large increase in translation activity of PDCAT upon the addition of the 3′ nontranslated RV sequence (PDCATSL4 RNA), demonstrated the ability of the RV 3′(+)SL and flanking sequences to enhance overall translational activity (Fig. 2). In addition, we tested the ability of the 3′ nontranslated RV sequence to enhance translation from alternative RV initiation codons. pPDCATSL6 contains a single nucleotide deleted from the RV 5′ sequence domain in pPDCATSL5, moving the AUG (nt 41) out of the CAT ORF and placing the AUG (nt 57) in frame with the CAT ORF (Fig. 1). Translation of PDCATSL6 RNA in the reticulocyte lysate system produced

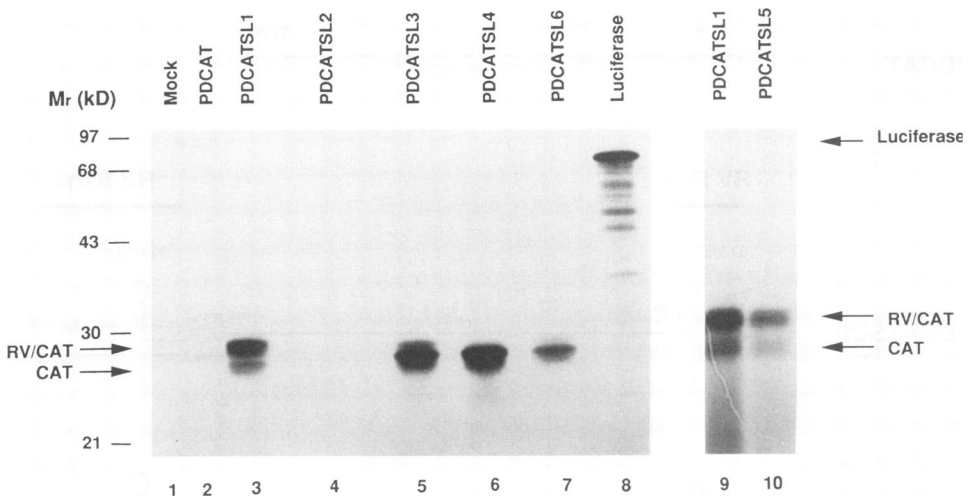

FIG. 2. Total in vitro translation products of chimeric RV/CAT RNAs. Lane 1, no RNA; lanes 2 to 7 and 9 to 10, translational products from indicated transcribed RNAs incubated in a rabbit reticulocyte lysate translation system (Promega) and separated by SDS-PAGE (12% polyacrylamide). Lanes 9 and 10 were derived from an SDS-PAGE gel separate from that containing lanes 1 to 8. Lane 8 shows the results of a control translation assay with luciferase RNA. Representative data from four independent experiments are shown.

a protein product pattern identical to that produced by PDCATSL3 RNA, but at a level 65% less (Fig. 2, lane 7; Table 1). In additional experiments, in vitro translation products from PDCATSL1 and derivative mutant RNAs were immunoprecipitated with antibodies raised against the CAT coding sequence. The profile of immunoprecipitated proteins was the same as that observed in Fig. 2, except for PDCAT, in which no protein was immunoprecipitated (36). These in vitro data demonstrate that the RV 5′ and 3′ sequences stimulate translation and, when present in *cis*, additively enhance initiation from RV-encoded initiation codons. In addition, the AUG codon present at nt 41 of the RV 5′-terminal sequence was the preferred site of translation initiation (Table 1).

The kinetics of [^{35}S]methionine incorporation for each RNA construct were monitored during the course of the 60-min in vitro translation reactions. Although the absolute levels of incorporation between constructs tested differed, the kinetic profiles were virtually identical, except for the essentially nonfunctional PDCAT and PDCATSL2 RNAs (36). These data suggested that the message stabilities were similar in vitro and that the quantitative differences in protein products truly reflect differential template translatability.

Role of the RV *cis*-acting elements in the translation of RV/CAT chimeric RNAs in vivo. The chimeric RV/CAT constructs (Fig. 1) were cloned into a pD5 vector which directs RNA expression in transfected mammalian cells by the adenovirus major late promoter. The DNA constructs were transfected into Vero 76 cells, and CAT activity was measured at different time periods after transfection. Initial studies indicated that the maximal level of CAT activity generated by these constructs was reached 24 h posttransfection (hpt), with a plateau in activity maintained through 48 hpt (36). This saturation of measurable CAT activity probably reflects the accumulation and stability of the CAT enzyme within transfected cells. We further investigated the translational activity of PDCATSL1, PDCATSL4, and PDCATSL5 RNA in vivo at time points within the linear range of CAT activity. These constructs were chosen for focused studies because they contained both 5′ and 3′ RV-terminal sequence domains, or deletions of either the entire 5′(+)SL or 3′(+)SL structures. CAT activity 12 hpt derived from cells transfected with PDCATSL1 vector was three times greater than that present in cells transfected with PDCATSL5 vector and was five times greater than that of cells expressing PDCATSL4 RNA (Fig. 3A). Cells transfected with the PDCATSL4 vector, which lacks the 5′ RV sequence domain, produced approximately half the CAT activity at 24 hpt observed in cells expressing PDCATSL1 and PDCATSL5, both of which contain the 5′ RV sequence (Fig. 3A). This observation contrasted with our previous results in vitro, in which PDCATSL4 RNA generated CAT protein at a level comparable with that of PDCATSL5 (Table 1). The greater ability of RNAs containing the 5′-terminal sequence of RV (PDCATSL1 and PDCATSL5) to generate CAT activity in vivo, compared with RNAs lacking this domain (PDCATSL4), indicated that this 5′ element was the primary stimulant of RV-initiated translation in vivo. These data also

TABLE 1. Quantitation of RV/CAT and CAT proteins synthesized from PDCAT and derivative chimeric RNAs in rabbit reticulocyte lysates[a]

Protein	Level of translation (optical density area) for[b]:						
	PDCAT	PDCATSL1	PDCATSL2	PDCATSL3	PDCATSL4	PDCATSL5	PDCATSL6
RV[c]		6.3	ND	2.2		2.6	0.58
CAT[d]	0.16	1.9	ND	8.5	5.9	1.4	3.9

[a] The ratios (average derived from two independent experiments) of translation products (RV/CAT) are as follows: PDCAT, 0:1; PDCATSL1, 3.2:1; PDCATSL2, not detectable (ND); PDCATSL3, 0.26:1; PDCATSL4, 0:1; PDCATSL5, 2:1; PDCATSL6, 0.2:1.
[b] Representative data (derived by laser densitometry) from one experiment.
[c] Translation products initiated from RV-encoded AUG codons.
[d] Translation products initiated from CAT-encoded AUG codon.

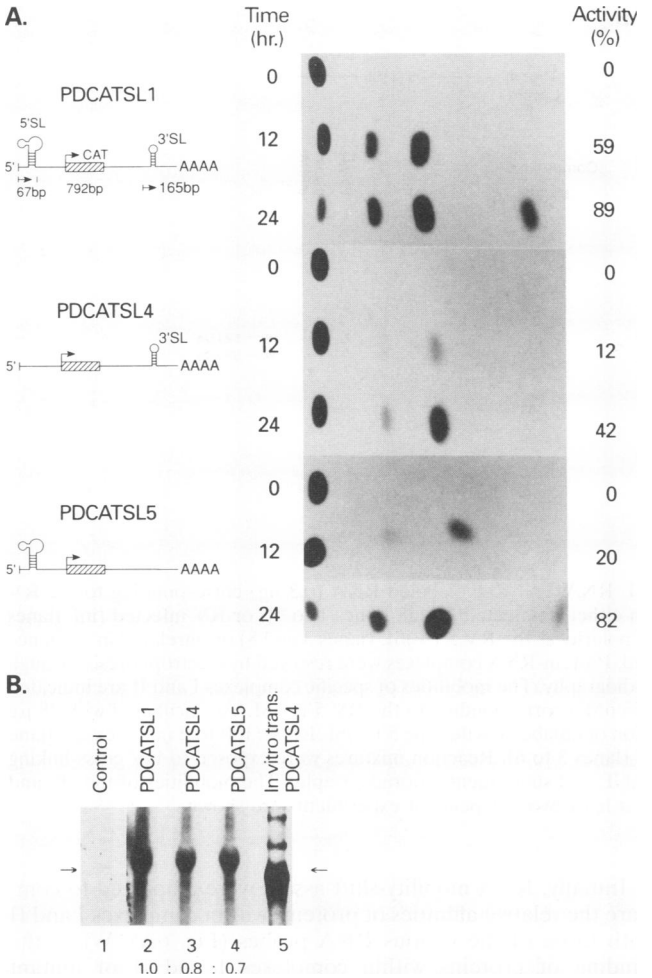

FIG. 3. (A) Functional analysis of the 5′ and 3′ SL sequences of RV RNA in transfected cells. DNA from three constructs, PDCATSL1, PDCATSL4, and PDCATSL5, was transfected into Vero 76 cells with lipofectin. CAT activity was measured from cells at 0, 12, and 24 h after transfection. The percentage of activity of each construct was derived by quantitating the conversion of [^{14}C]chloramphenicol from nonacetylated to both mono- and diacetylated forms. Schematic diagrams of the three constructs are also shown. (B) Northern blot analysis of total RNA (50 μg) from Vero 76 cells 24 h after transfection with PDCATSL1, PDCATSL4, and PDCATSL5 DNAs. Lane 1, RNA from nontransfected cells; lane 2, RNA from PDCATSL1-transfected cells; lane 3, RNA from PDCATSL4-transfected cells; lane 4, RNA from PDCATSL5-transfected cells; lane 5, in vitro-transcribed RNA (5 ng) from the PDCATSL4 vector. The ratios beneath lanes 3 and 4 allow comparison of the amount of hybridized signal quantitated in each sample standardized against PDCATSL1. These ratios are average values derived from three independent experiments. Arrows, expected size of RNAs.

confirmed the previous observations that both the 5′ and 3′ structures are required for achieving maximal translation activity.

To ensure that the observed differences in CAT activity in vivo were not due to variations in RNA transcription or stability, Northern blot analysis was performed with RNA extracted from cells transfected with the above constructs at various times posttransfection. Differences in RV/CAT mRNA levels produced by the three constructs were noted 24 hpt (Fig. 3B, lanes 2 to 4). Although PDCATSL4- and PDCATSL5-transfected cells contain comparable amounts of RNA at 24 hpt (Fig. 3B, compare lanes 3 and 4), cells transfected with PDCATSL5 exhibited twice the CAT activity as those expressing PDCATSL4 (Fig. 3A). The lack of correlation of CAT activity and RNA level is also seen when comparing the essentially equivalent levels of CAT activity 24 hpt (Fig. 3A) in cells transfected with PDCATSL1 and PDCATSL5, in which some differences in RNA levels were observed. These results suggested that RNA stability was not a major determinant of the observed differences in RNA translation. No hybridization occurred with RNA extracted from nontransfected Vero 76 cells (Fig. 3B, lane 1). The broad nature of the hybridized bands corresponding to the RV/CAT mRNAs reflects their comigration with the 18S rRNA and the large amount of RNA required to visualize these chimeric RNAs. In vitro-transcribed RNA from the pPDCATSL4 vector was used as a marker to identify the approximate size of the in vivo-transcribed RNA (Fig. 3B, lane 5). Increase in the size of in vivo-transcribed RNA is due to the presence of simian virus 40 polyadenylation sequences at the 3′ end.

Characterization of host protein interactions with the RV 5′(+)SL structure. Both in vitro and in vivo translation assays showed that the presence of both 5′- and 3′-terminal sequences of RV RNA efficiently enhanced the translation of RV/CAT chimeric RNAs (Fig. 2 and 3A). Although PDCATSL4 RNA, which lacks the 5′ RV SL sequences, was an efficient template for in vitro translation (Table 1), it consistently generated only half the level of CAT activity in transfected Vero 76 cells generated by PDCATSL1 and PDCATSL5, which both contain this structure (Fig. 3A). The lack of agreement between these assay systems suggested that the RV 5′-terminal RNA sequence was recognized by components of the Vero 76 cell-encoded translation system or associated factors. We investigated this possibility by synthesizing uniformly radiolabeled RNA molecules encompassing the 5′(+)SL structure and incubating this probe with cytosolic extracts derived from uninfected and RV-infected Vero 76 cells. RNA-binding proteins present in these extracts were visualized by RNA gel-shift assays and UV cross-linking techniques (Fig. 4). Several preparations of cytolysates were tested for their ability to bind RV 5′(+)SL RNA to ensure consistency of results and to control for artifactual interactions.

Incubation of radiolabeled 5′(+)SL RNA with cytolysates derived from mock-infected or RV-infected Vero 76 cells resulted in four RNA-protein complexes (Fig. 4A, lanes 2 and 7). Increasing amounts of specific and nonspecific RNAs were used for the competition assays. Upon the addition of 100-fold molar excess of unlabeled RNA of identical sequence and polarity, the binding of proteins within complexes I and II was reduced by >90% in either infected or uninfected lysates (Fig. 4A, lanes 3 and 8). Addition of unrelated RNAs such as globin and poly(I-C) resulted in only modest reductions in these complexes (Fig. 4A, lanes 5, 6, 10, and 11). Interestingly, addition of one RNA species, hY3RNA, a low-abundance RNA present in cytoplasmic ribonucleoprotein complexes (40), did selectively compete (>85%) for the binding of proteins within complexes I and II (Fig. 4A, lanes 4 and 9). In contrast to the consistent and specific pattern of binding seen with these complexes (I and II), other slower-migrating complexes showed no specificity and varied in their intensity, depending on the preparation of the cytolysates (Fig. 4A).

In order to ascertain the nature of the binding proteins within the Vero 76 cytolysates, complexes from 5′(+)SL RNA mobility-shift assays were exposed to UV light and products were resolved by SDS-PAGE. Two major proteins ~59 and 52 kDa in size were found to specifically interact with the

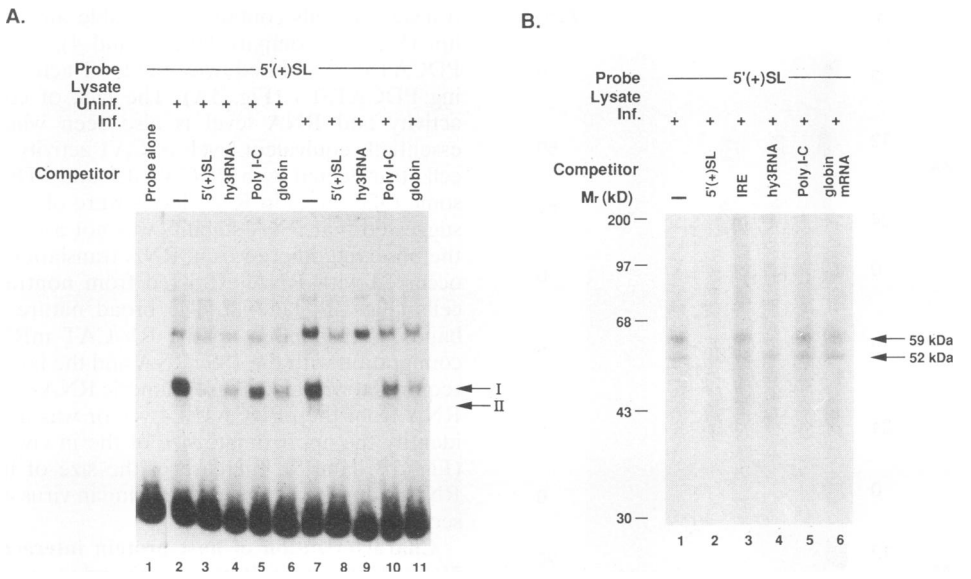

FIG. 4. Specific binding of cytosolic proteins to the RV-encoded 5′(+)SL RNA. (A) Radiolabeled RNA (0.3 ng) corresponding to the RV 5′(+)SL structure was incubated with 20 μg of cytosolic lysates derived from either uninfected (uninf. [lanes 1 to 6]) or RV-infected (inf. [lanes 7 to 11]) cells. Unlabeled competitor RNAs, either of the same sequence and polarity as the RV 5′(+)SL (lanes 3 and 8) or unrelated in sequence (lanes 4 to 6 and 9 to 11), were supplied at 100-fold molar excesses as indicated. Protein-RNA complexes were resolved by electrophoresis through a 6% polyacrylamide gel in Tris-borate-EDTA buffer and visualized by autoradiography. The mobilities of specific complexes I and II are indicated at the right. Free probe is seen in lane 1. (B) Radiolabeled RNA (0.7 ng [3.55 nM]) corresponding to the RV 5′(+)SL was incubated with 28 μg of cytosolic lysates derived from infected cell lysates (lane 1) or with the addition of unlabeled wild-type 5′(+)SL RNA (100-fold molar excess [lane 2]) or the indicated unrelated RNAs, each supplied at 100-fold molar excess (lanes 3 to 6). Reaction mixtures were exposed to UV cross-linking procedures, and proteins bearing transferred label were resolved by SDS-PAGE and subsequent autoradiography. The mobilities of the 59- and 52-kDa proteins are indicated by arrows at right. Representative data from at least two independent experiments are shown.

radiolabeled 5′(+)SL RNA probe when incubated with either uninfected or infected cellular lysates (Fig. 4B). The ratio of 59- to 52-kDa proteins binding the 5′(+)SL structure was generally 1.4:1, but some variation between lysate preparations was observed. A 100-fold molar excess of RNA identical in sequence and polarity specifically reduced (~90%) the binding of the 59- and 52-kDa proteins to the labeled 5′(+)SL RNA (Fig. 4B, compare lanes 1 and 2). Indeed, only 25-fold molar excess of the unlabeled 5′(+)SL RNA was required to achieve similar (>80%) reductions in protein binding. Unrelated RNAs, such as the iron-responsive element, poly(I-C), and globin RNA, when supplied at a 100-fold molar excess, reduced binding of the 59- and 52-kDa proteins to the labeled RV 5′(+)SL RNA by an average of ~26% (Fig. 4B, lanes 3, 5, and 6). These results, coupled with those in Fig. 4A, established the specificity of the interactions between the 59- and 52-kDa proteins and the labeled RV 5′(+)SL RNA. However, hY3RNA did selectively compete for the binding of the 59-kDa protein, reducing its level by 73% (Fig. 4B, lane 4). The level of competition was dependent on the amount of unlabeled RNA included in a given assay. Essentially identical results were obtained when uninfected cell lysates containing radiolabeled 5′(+)SL were exposed to UV light and subsequently challenged with unlabeled RNAs.

Identification of the protein binding site(s) within the 5′(+)SL RNA. In order to tentatively localize the binding site(s) of 59- and 52-kDa proteins within the 5′(+)SL, a series of mutant SL structures were constructed in which certain stem regions of the 5′(+)SL were destabilized or single-stranded bulge regions were removed (Fig. 5). Radiolabeled RNAs corresponding to each of these structures were transcribed in vitro and their ability to bind cytosolic proteins was compared with the binding ability of the wild-type RV 5′(+)SL RNA.

Initially, RNA mobility-shift assays were employed to compare the relative affinities of proteins within complexes I and II with those of the various RNA probes (Fig. 6A). When the binding of proteins within complexes I and II of mutant 5′(+)SL-m1 (Fig. 5), which lacks the SL region containing AUG (nt 41), was investigated with uninfected and RV-infected lysates, the amounts of material present within these complexes were 77 and 64%, respectively, of that bound by the wild-type 5′(+)SL RNA (Fig. 6A, lanes 3 and 10). Deletion of three adenosines within a loop region (Fig. 5) created 5′(+)SL-m3, which was bound by proteins in complexes I and II equally as well as the wild-type RNA in repeated experiments (Fig. 6A, lanes 4 and 11).

Mutants containing alterations in the terminal stem region of the 5′(+)SL structure [5′(+)SL-m6, -m7, and -m9 (Fig. 5)] displayed disparate binding affinities for host-encoded proteins. Upon incubation of 5′(+)SL-m6 RNA with cytolysates from mock- or RV-infected cells, complexes I and II contained ~35% of the amount of bound RNA, as seen with the wild-type RNA (Fig. 6A, lanes 5 and 12). In contrast, addition of mutant RNAs 5′(+)SL-m7 and -m9, each predicted to contain increased single-stranded RNA character (Fig. 5), to the binding assays resulted in >250 and >220% increases in bound RNA within complexes I and II, respectively, compared with the wild-type 5′(+)SL RNA (Fig. 6A, lanes 6, 7, 13, and 14). The 5′(+)SL-m6 mutant contains a single base mutation removing the single-stranded bulge region in the terminal stem region of the 5′(+)SL structure (Fig. 5). However, destabilization of either the upper portion of the terminal stem (m9) or the lower portion (m7) of the 5′(+)SL structure is predicted to result in larger single-stranded RNA domains (Fig. 5). The differential levels of binding observed with mutants 5′(+)SL-m6, -m7, and -m9 (Fig. 6A), compared with that of the

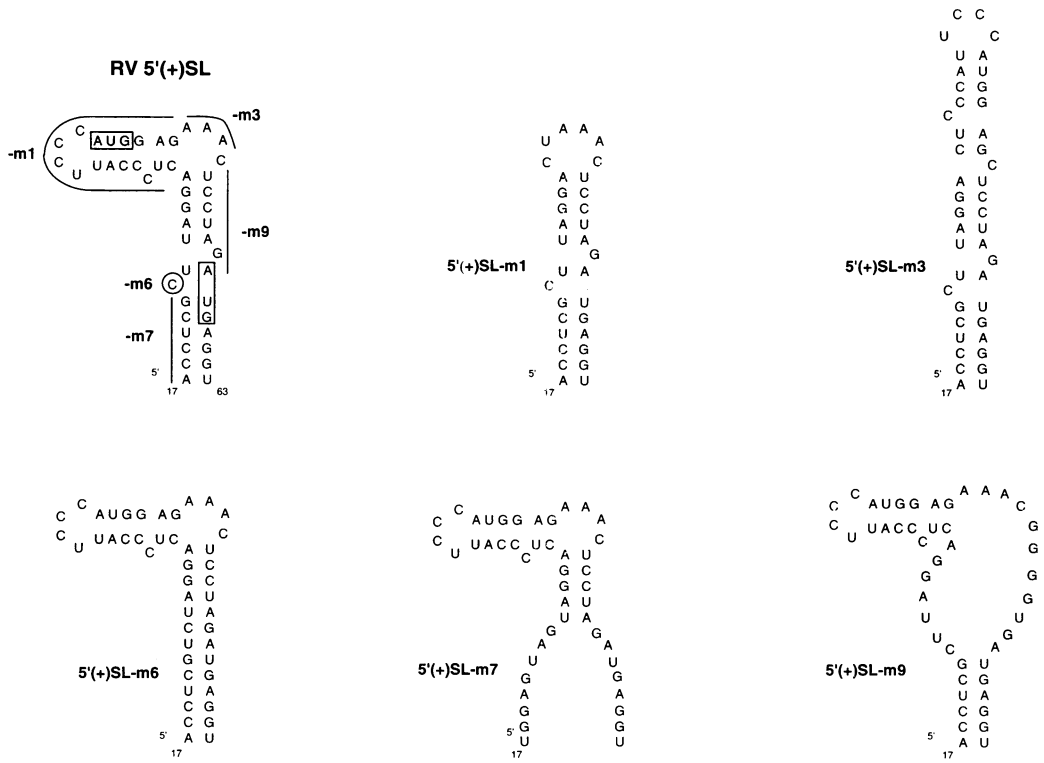

FIG. 5. Predicted structures of the RV 5′(+)SL and derivative mutants. Specific domains affected by each of the derivative mutants are indicated on the wild-type RV 5′(+)SL by lines or circled nucleotides. The numbering of nucleotides within the wild-type and mutant SL structures corresponds to those present within the RV genome (5). AUGs present at nt 41 and 57 are boxed in the wild-type structure. 5′(+)SL-m1 contains a deletion of nt 32 to 46, while 5′(+)SL-m3 bears a deletion of nt 37 to 40. The un-base-paired cytosine at position 23 was removed and placed at nt 25 in 5′(+)SL-m6, thereby removing the single-strand RNA bulge region within the terminal stem region. A predicted destabilization of the lower portion of the terminal stem resulting from substitutions in nt 17 to 24 is contained within 5′(+)SL-m7. Mutant 5′(+)SL-m9 contains substitutions in nt 51 to 57, which are predicted to destabilize regions in the upper region of the terminal stem within these structures.

wild-type 5′(+)SL RNA, suggested that the terminal stem, including the bulge region, of the 5′(+)SL comprised an area in which the binding proteins present in complexes I and II interact. It should be noted that increased amounts of mutant RNAs 5′(+)SL-m3, -m6, -m7, and -m9 were bound within slower-migrating protein-RNA complexes known to be not specific for wild-type 5′(+)SL RNA (Fig. 6A).

We wished to determine the ability of mutant probes to be bound by the 59- and 52-kDa cellular proteins, which specifically interact with the wild-type 5′(+)SL RNA. Radiolabeled wild-type RV 5′(+)SL and the derivative 5′(+)SL-m6 and -m9 mutant probes were individually incubated with cell lysates, and the resulting protein-RNA complexes were visualized after treatment with UV light and SDS-PAGE analysis (Fig. 6B). The amounts of the 59- and 52-kDa proteins present in complexes containing each of the mutant probes were compared with that of the wild-type RV 5′(+)SL RNA. The amount of 59- and 52-kDa proteins present in RNA-protein complexes was 150% greater when incubated with 5′(+)SL-m9 RNAs than the amount in those containing the wild-type probe (Fig. 6B, compare lane 2 with lane 1). A similar increase in binding affinity of the 59- and 52-kDa proteins was also seen for 5′(+)SL-m7, which is predicted to contain a destabilization in the terminal stem region. This result was in agreement with their enhanced abilities to bind proteins contained in complexes I and II in RNA mobility-shift assays, although absolute values differed (Fig. 6A, lanes 6, 7, 13, and 14). Overall binding of the 59- and 52-kDa proteins to the 5′(+)SL-m6 probe, which was predicted to contain no single-stranded character in the terminal stem region (Fig. 5), was only 41% of the amount bound by the wild-type probe (Fig. 6B, lane 3). This effect on binding was in accord with its relatively poor ability to be bound in complexes I and II in RNA mobility-shift assays (Fig. 6A, lanes 5 and 12). It should be noted that few proteins corresponding to the nonspecific, slower-migrating RNA-protein complexes were seen in UV cross-linking assays (compare Fig. 6A with 6B).

Partial identification of proteins which interact with the 5′(+)SL structure. It was curious to note that hY3RNA reduced the binding of the 59-kDa protein to the RV 5′(+)SL probe by >85 and 73% in RNA mobility-shift and UV cross-linking assays, respectively (Fig. 4A, lanes 4 and 9, and 4B, lane 4). Furthermore, comparison of the 5′(+)SL RNA sequences with those from hYRNAs (40) revealed limited regions of sequence similarity (Fig. 7A) surrounding a conserved single-stranded bulge region containing an un-base-paired cytosine residue (Fig. 7A). It is known that the cytosine-containing RNA bulge regions present in the hYRNAs are bound by a set of cytoplasmic proteins known as the Ro/SS-A antigen (40), the predominant protein within this complex having a molecular mass of 60 kDa (4, 17, 29, 37, 40). Interestingly, removal of the cytosine-containing bulge from the RV mutant 5′(+)SL-m6 RNA (Fig. 5) reduced binding of the 59- and 52-kDa proteins by as much as 65% (Fig. 6A, lanes 5 and 12). On the basis of the ability of hY3RNA to efficiently compete with the RV 5′(+)SL probe for 59-kDa protein

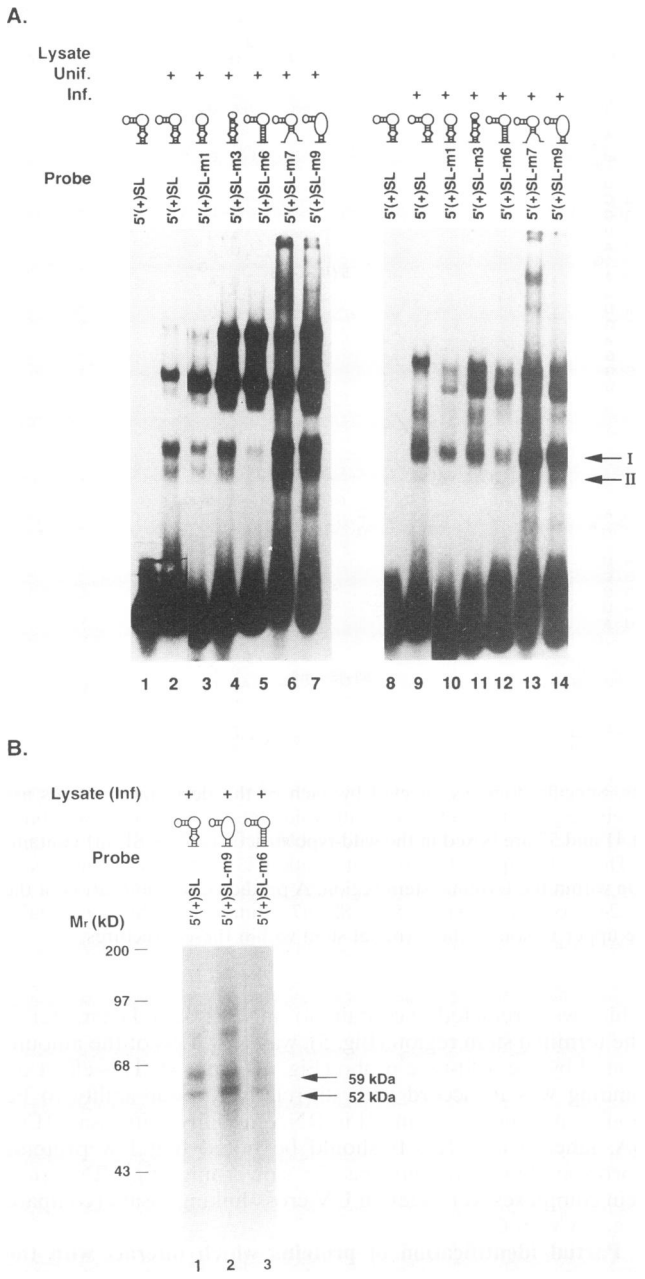

FIG. 6. Comparison of host-encoded protein binding to radiolabeled wild-type RV 5′(+)SL and derivative mutant RNAs. (A) Radiolabeled RNA (0.3 ng) corresponding to RV 5′(+)SL (lanes 2 and 9), 5′(+)SL-m1 (lanes 3 and 10), 5′(+)SL-m3 (lanes 4 and 11), 5′(+)SL-m6 (lanes 5 and 12), 5′(+)SL-m7 (lanes 6 and 13), and 5′(+)SL-m9 (lanes 7 and 14) were incubated with 20 μg of cytosolic lysates derived from either uninfected (Uninf. [lanes 2 to 7]) or RV-infected (Inf. [lanes 9 to 14]) cells. Protein-RNA complexes were resolved as described in the legend to Fig. 4 and Materials and Methods. Free probe is seen in lanes 1 and 8. The positions of specific complexes I and II are indicated to the right. Schematic drawings of the predicted structures of the radiolabeled RNA probes are shown above the appropriate lanes. Representative data from two independent experiments are shown. (B) The indicated radiolabeled RNAs, wild-type RV 5′(+)SL (lane 1), 5′(+)SL-m6 (lane 2), and 5′(+)SL-m9 (lane 3) were incubated with 28 μg of RV-infected lysates and exposed to UV cross-linking procedures. RNA-protein complexes were resolved by SDS-PAGE (10% polyacrylamide) and subsequent autoradiography. Schematic drawings of the predicted structures of the radiolabeled RNA probes are shown above the appropriate lanes. The arrows indicate the positions of the 59- and 52-kDa proteins.

binding and the structural similarities of the protein binding domains within these RNA structures, we tested whether the 59- and 52-kDa proteins are related to proteins comprising the Ro/SS-A antigen or other autoantigens.

Cytosolic proteins from both uninfected and RV-infected cell lysates were covalently cross-linked to labeled 5′(+)SL RNA by exposure to UV light, and the resulting RNA-protein complexes were immunoprecipitated with Ro-type human polyclonal serum (Ge), which was derived from individuals suffering from autoimmune disorders (2, 2a). Proteins obtained after these immunoprecipitation reactions were resolved by SDS-PAGE. This human Ro-type serum immunoprecipitated labeled 59- and 52-kDa proteins from binding reaction mixtures containing the radiolabeled RV 5′(+)SL RNA probe (Fig. 7B, lanes 3 and 4). The presence of a 52-kDa protein in immunoprecipitations from uninfected lysates can be seen upon longer exposure (Fig. 7B, lane 3). No proteins were immunoprecipitated when the 5′(+)SL-protein complexes were incubated with either human serum from individuals not suffering from autoimmune disorders (normal serum [Fig. 7B, lanes 1 and 2]) or serum raised against an unrelated protein, such as calreticulin (Fig. 7B, lanes 5 and 6). In addition, human Ge antiserum did not immunoprecipitate proteins associated with RNA probes derived from other portions of the RV genome (36). These data suggested that the 59- and 52-kDa proteins binding the RV 5′(+)SL RNA are either antigenically related to Ro/SS-A antigens or make up a distinct set of autoimmune antigens.

In order to determine whether these binding proteins corresponded to known components of the Ro/SS-A complex, immunoprecipitation reactions were performed with the monoclonal antibody A6, polyclonal antiserum generated against recombinant 60-kDa Ro protein, and polyclonal antiserum 6739 raised against the recombinant 52-kDa component of the Ro complex. In order to qualify the antibodies, [^{35}S]methionine-labeled proteins from mock and RV-infected cells were immunoprecipitated with various antisera. The expected proteins were precipitated by antisera in the absence of any RNA probe (36). Duplicate immunoprecipitations were performed (Fig. 7B, lanes 7 to 17) with lysates incubated with either 5′(+)SL RNA or hY3RNA, a native substrate for Ro protein binding. Preimmune (normal) serum did not immunoprecipitate any RNA-protein complexes after exposure of lysates containing radiolabeled hY3RNA to UV light (Fig. 7B, lane 13). With a polyclonal antiserum raised against recombinant 60-kDa Ro protein, protein-hY3RNA complexes ~68 and 60 kDa in size were immunoprecipitated (Fig. 7B, lane 14). Interestingly, monoclonal antiserum raised against a 60-kDa Ro protein immunoprecipitated predominant complexes containing hY3RNA ~71 and 48 kDa in size (Fig. 7B, lane 15). Human Ro-type serum (Ge) immunoprecipitated a protein complex containing hY3RNA 68 kDa in size and less-reactive complexes ~60 and 48 kDa in size (Fig. 7B, lane 17). Antiserum raised against recombinant 52-kDa Ro protein showed little reactivity (Fig. 7B, lane 16). At present, the reasons for the observed differences in the molecular masses of protein-hY3RNA complexes precipitated by monoclonal antibody A6 and other Ro antisera are not clear.

In contrast to results with hY3RNA, in repeated experiments, only human polyvalent serum (Ge) was found to immunoprecipitate protein-RNA complexes containing RV

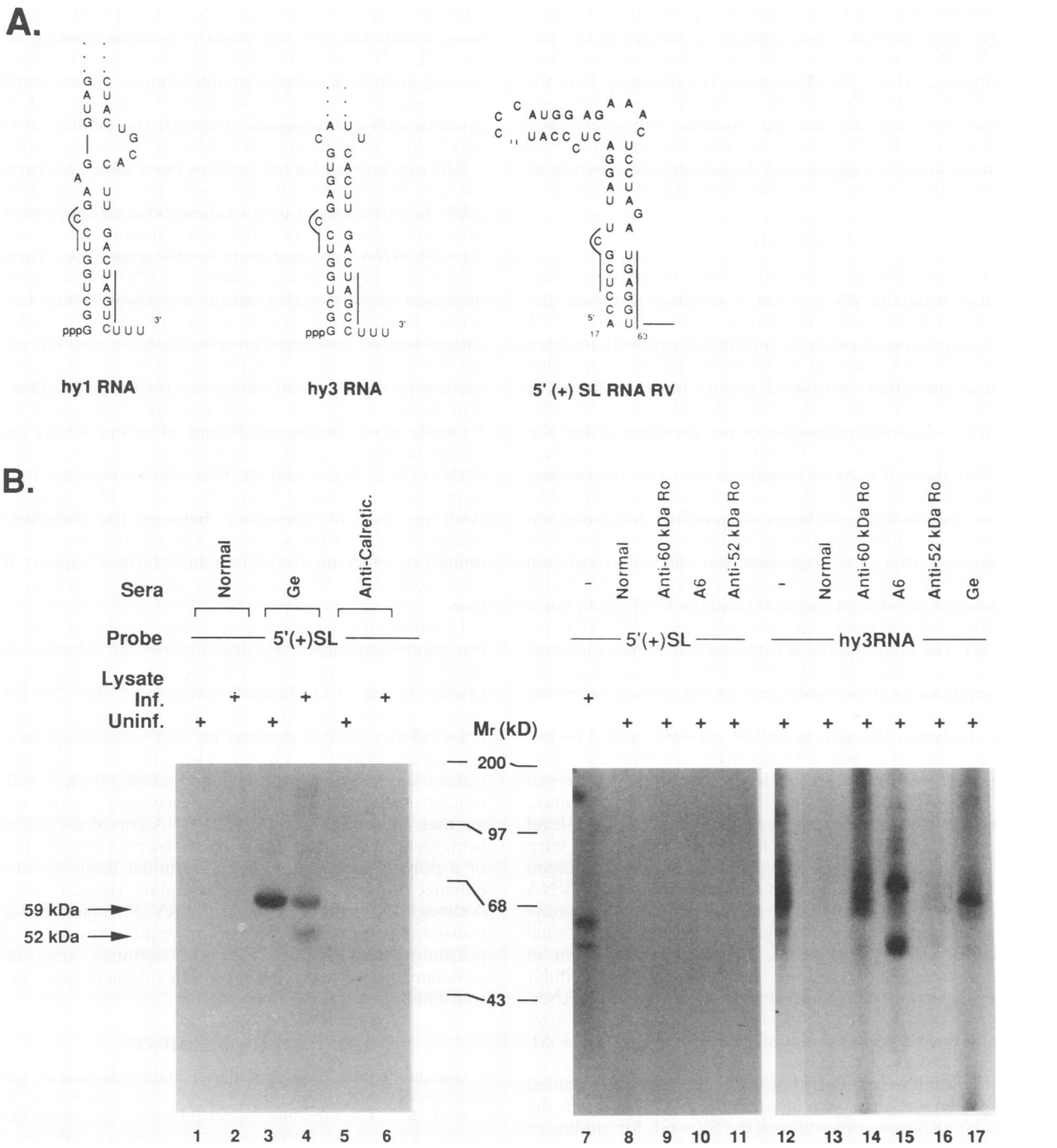

FIG. 7. (A) Comparison of sequence and predicted structural similarities between the RV 5′(+)SL and the terminal stem region of hY1RNA and hY3RNA (40). Lines indicate regions of similarity shared by these RNAs. (B) Immunoprecipitation of RNA-protein complexes containing radiolabeled RV 5′(+)SL and hY3RNA. Uninfected (Uninf.) and RV-infected (Inf.) cell lysates (60 μg) were incubated with radiolabeled RV 5′(+)SL (1.4 ng) and subjected to UV cross-linking procedures followed by immunoprecipitation with (normal) human serum from patients not suffering from autoimmunity (lanes 1 and 2), human Ro-type polyclonal antiserum Ge (lanes 3 and 4), or polyclonal antibodies directed against N- and C-terminal peptides of human calreticulin (lanes 5 to 6). The mobilities of the 59- and 52-kDa proteins immunoprecipitated by Ge antiserum are indicated to the left. Immunoprecipitation data representative of at least three independent experiments are shown. Uninfected cell lysates (60 μg) were incubated with radiolabeled (1.4 ng) 5′(+)SL RNA (lanes 8 to 11) or hY3RNA (lanes 12 to 17) and subjected to UV cross-linking procedures followed by immunoprecipitation with the indicated antiserum: preimmune (normal) serum (lanes 8 and 13), polyclonal serum directed against the recombinant 60-kDa Ro antigen (lanes 9 and 14), monoclonal serum directed against the 60-kDa Ro/SS-A antigen (lanes 10 and 15), polyclonal antiserum specific for the recombinant 52-kDa Ro antigen (lanes 11 to 16), and human Ro-type polyclonal antiserum (lane 17). Immunoprecipitated proteins were resolved by SDS-PAGE (10% polyacrylamide) and subsequent autoradiography. Control UV cross-linking reaction mixtures containing 5′(+)SL (lane 7) and hY3RNA (lane 12) were not subjected to immunoprecipitation reactions and generally required fivefold less exposure than those involving immunoprecipitation.

5′(+)SL RNA (Fig. 7B, lanes 3 and 4). The inability of mono- and polyclonal antisera, raised against recombinant 60- and 52-kDa Ro/SS-A antigen components, to immunoprecipitate such complexes (Fig. 7B, lanes 9 to 11) indicates that the proteins binding the RV 5′(+)SL *cis*-acting element are not the known 60- and 52-kDa Ro proteins. However, their reactivity with antibodies derived from patients suffering from autoimmune diseases suggests that the binding proteins may be associated with or related to certain autoantigen complexes.

DISCUSSION

Results from both in vitro and in vivo translation assays demonstrate that the RV 5′- and 3′-terminal sequence domains efficiently promote translation of chimeric RV/CAT RNAs. Comparison of ratios of translation products initiated from RV- and CAT-encoded AUG codons (Table 1) revealed that translation initiates with much greater frequency from the RV-encoded AUG at nt 41 than with the AUG at nt 57. This preference is observed regardless of the presence of the RV 3′(+)SL sequence (Fig. 2). Therefore, the sequence context surrounding these RV AUG codons seems to be the primary factor dictating the preferential use of AUG (nt 41). The consensus sequence for the bases surrounding eucaryotic initiation codons contains a guanosine residue at the +4 position, which suggests that it is important for efficient translation (14–16). Indeed, this +4 guanosine is present immediately downstream of the RV AUG (nt 41) and the CAT AUG but is conspicuously absent from sequences adjacent to RV AUG (nt 57 [Fig. 5]). The ability of the RV-terminal sequence elements to enhance the translational suitability of heterologous coding regions emphasizes their importance in the translation of the RV nonstructural genes.

While analyzing the effects of RV 5′(+)SL and 3′(+)SL RNA sequences in directing translation, we observed differences in the levels of PDCATSL4 RNA translation in vitro and in vivo. PDCATSL4 RNA, which lacks the 5′(+)SL sequence, promoted CAT activity in vivo at only 20 to 50% of the level produced by PDCATSL1 RNA (Fig. 3). In contrast, in vitro studies showed that PDCATSL4 RNA produced translation products >70% the level observed with PDCATSL1 RNA (Fig. 2; Table 1). This lack of agreement between assays performed in vitro and in vivo suggested a greater translational enhancing role for the 5′(+)SL structure in vivo than in cell-free systems. Therefore, we sought to identify cellular proteins which specifically interact with the RV 5′(+)SL RNA. Indeed, two cellular protein species, 59 and 52 kDa in size, specifically bound the terminal stem region of the 5′(+)SL structure (Fig. 4 and 6).

Very few cellular proteins that interact with virus-encoded *cis*-acting elements have been identified (21, 27). However, the ability of hY3RNA to compete with the 5′(+)SL for binding of the 59-kDa protein (Fig. 4), coupled with similarities in their predicted structure and the approximate sites of protein binding (Fig. 7A), suggested that components of the Ro/SS-A antigen complex (4, 29, 37, 40) may be interacting with the 5′(+)SL RNA. Indeed, human Ro-type serum Ge (2, 2a) specifically immunoprecipitated 59- and 52-kDa proteins bound to radiolabeled RV 5′(+)SL RNA (Fig. 7B). Immunoprecipitation of protein-hY3RNA complexes by the human serum Ge confirmed its ability to recognize RNA binding proteins within the Ro/SS-A antigen complex (Fig. 7B). Further characterization of the RV 5′(+)SL RNA binding proteins revealed that poly- and monoclonal antisera raised against recombinant 60-kDa Ro antigen, which immunoprecipitated complexes containing hY3RNA, did not immunoprecipitate complexes containing the RV 5′(+)SL. These data suggest that the 59- and 52-kDa proteins binding the RV 5′(+)SL RNA are novel polypeptides. Further studies, employing additional samples of autoimmune patient serum, will be necessary to confirm the association of the 5′(+)SL binding proteins with autoantigens. However, the identity of the 59- and 52-kDa proteins will be established upon their purification.

The autoantigen La has recently been shown to correct and enhance translation initiation from the authentic poliovirus AUG in vitro (21). In light of these observations, the binding of host proteins reactive with human autoimmune serum to the 5′(+)SL RNA may contribute to RV translation. These proteins have a higher binding affinity for RNA probes containing increased single-stranded nature and lower affinity for RNA probes lacking single-stranded domains (Fig. 6). Such observations suggest that these proteins could be involved in destabilizing or unwinding 5′ NTR secondary structure elements, thereby providing an attractive site for the translation initiation. Interestingly, the complementary sequence of the RV 5′(+)SL RNA (anti-sense strand of virion RNA) exerts a strong inhibitory effect on translation from the CAT AUG (PDCATSL2; Fig. 1 and 2). It is also known that this RNA sequence is not bound by the 59- and 52-kDa proteins (24). Both the lack of interaction between the complementary strand of the 5′(+)SL sequence with the host proteins and its inhibitory effect on translation may further support the involvement of the 59- and 52-kDa cellular proteins in translation.

Initiation of translation from either the RV or CAT AUGs was greatly enhanced (>37-fold in vitro and 3-fold in vivo) by the presence of the RV 3′(+)SL sequences and poly(A) tract (Table 1; Fig. 3A). Indeed, removal of the 3′(+)SL and immediate flanking sequences, leaving the poly(A) tract intact (PDCATSL5 RNA), resulted in >50% reduction in overall translation (Table 1; Fig. 2). The additive enhancement in translation observed from RNAs containing both 5′ and 3′ SL structures suggests that these sequences may interact with one another. However, no regions of RNA complementarity have been identified to date. It has been observed that the presence of a poly(A) tract and other 3′-terminal sequence elements enhance mRNA stability and stimulate translation (9, 10). Although the manner in which the RV 3′ sequences augment translation is presently unclear and requires further study, the possibility exists that RV 5′- and 3′-terminal structures may associate in vivo via protein-protein interactions to promote translation.

ACKNOWLEDGMENTS

Giovanna Tosato, Gerardo Kaplan, and Barry Falgout are gratefully acknowledged for their critical review of the manuscript. We also thank E. K. L. Chan (Scripps Research Institute) for providing human Ro-type serum (Ge), monoclonal serum against recombinant 60-kDa Ro, and polyclonal antiserum raised against recombinant 52-kDa Ro. We gratefully acknowledge R. D. Sontheimer (University of Texas Southwestern Medical Center) for providing human anti-calreticulin peptide serum, Jack Keene and Ameeta Kelkar (Duke University Medical Center) for polyclonal serum raised against recombinant 60-kDa Ro protein, and Sandra Wolin (Yale University) for the gift of the pT7hY3RNA plasmid DNA. We thank John Ewell for the synthesis of oligonucleotides.

REFERENCES

1. **Andino, R., G. E. Rieckhof, and D. Baltimore.** 1990. A functional ribonucleoprotein complex forms around 5′ end of the poliovirus RNA. Cell **63**:369–380.
2. **Ben-Chetrit, E., E. K. L. Chan, K. F. Sullivan, and E. M. Tan.** 1988. A 52 kD protein is a novel component of the SS-A/Ro

antigenic particle. J. Exp. Med. **167**:1560–1571.
2a. **Chan, E. K. L., J. C. Hamel, J. P. Buyon, and E. M. Tan.** 1991. Molecular definition and sequence motifs of the 52-kDa component of human SS-A/Ro autoantigen. J. Clin. Invest. **87**:68–76.
3. **del Angel, R. M., A. G. Papavassiliou, C. Fernandez-Thomas, S. J. Silverstein, and V. R. Racaniello.** 1989. Cell proteins bind to multiple sites within the 5′ untranslated region of poliovirus RNA. Proc. Natl. Acad. Sci. USA **86**:8299–8303.
4. **Deutscher, S. L., J. B. Harley, and J. D. Keene.** 1988. Molecular analysis of the 60 kDa human Ro ribonucleoprotein. Proc. Natl. Acad. Sci. USA **85**:9479–9483.
5. **Dildine, S. L., and B. L. Semler.** 1992. Conservation of RNA-protein interactions among picornaviruses. J. Virol. **66**:4364–4376.
6. **Dominguez, G., C.-Y. Wang, and T. K. Frey.** 1990. Sequence of the genome RNA of rubella virus: evidence for genetic rearrangement during togavirus evolution. Virology **177**:225–238.
7. **Dreher, T. W., A. L. N. Rao, and T. C. Hall.** 1989. Replication in vivo of mutant brome mosaic virus RNAs defective in aminoacylation. J. Mol. Biol. **206**:425–438.
8. **Duke, G. M., M. A. Hoffman, and A. C. Palmenberg.** 1992. Sequence and structural elements that contribute to efficient encephalomyocarditis virus RNA translation. J. Virol. **66**:1602–1609.
9. **Gallie, D. R.** 1991. The cap and poly (A) function synergistically to regulate mRNA translational efficiency. Genes Dev. **5**:2108–2116.
10. **Gallie, D. R., J. N. Feder, R. T. Schimke, and V. Walbot.** 1991. Functional analysis of the tobacco mosaic virus tRNA-like structure in cytoplasmic gene regulation. Nucleic Acids Res. **19**:5031–5036.
11. **Haller, A. A., and B. L. Semler.** 1992. Linker scanning mutagenesis of the internal ribosome entry site of poliovirus RNA. J. Virol. **66**:5075–5086.
12. **Jang, S. K., T. V. Pestova, C. U. T. Hellen, G. W. Witherell, and E. Wimmer.** 1990. Cap-independent translation of picornavirus RNAs: structure and function of the internal ribosomal entry site. Enzyme **44**:292–309.
13. **Jang, S. K., and E. Wimmer.** 1990. Cap-independent translation of encephalomyocarditis virus RNA: structural element of the internal ribosomal entry site and involvement of a cellular 57-kD RNA binding protein. Genes Dev. **4**:1560–1572.
14. **Kozak, M.** 1986. Point mutations define a sequence flanking the AUG initiator codon that modulates translation by eukaryotic ribosomes. Cell **44**:283–292.
15. **Kozak, M.** 1989. Context effects and inefficient initiation at non-AUG codons in eucaryotic cell-free translation systems. Mol. Cell. Biol. **9**:5073–5080.
16. **Kozak, M.** 1989. Circumstances and mechanisms of inhibition of translation by secondary structure in eucaryotic mRNAs. Mol. Cell. Biol. **9**:5134–5142.
17. **Lerner, M. R., J. A. Hardin, and J. A. Steitz.** 1981. Two novel classes of small ribonucleoproteins detected by antibodies associated with lupus erythematosus. Science **211**:400–402.
18. **McCauliffe, D. P., E. Zappi, T. S. Lui, M. Michalak, R. D. Sontheimer, and J. D. Capra.** 1990. A human Ro/SS-A autoantigen is the homologue of calreticulin and is highly homologous with Onchoceral RAL-1 antigen and an Aplysia "memory molecule." J. Clin. Invest. **86**:332–335.
19. **Meerovitch, K., R. Nicholson, and N. Sonenberg.** 1991. In vitro mutational analysis of *cis*-acting RNA translational elements within the poliovirus type 2 5′ untranslated region. J. Virol. **65**:5895–5901.
20. **Meerovitch, K., J. Pelletier, and N. Sonenberg.** 1989. A cellular protein that binds to the 5′ noncoding region of poliovirus RNA: implications for internal translation initiation. Genes Dev. **3**:1026–1034.
21. **Meerovitch, K., Y. V. Svitkin, H. S. Lee, F. Lejbkowicz, D. J. Kenan, E. K. L. Chan, V. I. Agol, J. D. Keene, and N. Sonenberg.** 1993. La autoantigen enhances and corrects aberrant translation of poliovirus RNA in reticulocyte lysate. J. Virol. **67**:3798–3807.
22. **Milligan, J. F., D. R. Groebe, G. W. Witherell, and O. C. Uhlenbeck.** 1987. Oligoribonucleotide synthesis using T7 RNA polymerase and synthetic DNA templates. Nucleic Acids Res. **15**:8783–8798.
23. **Najita, L., and P. Sarnow.** 1990. Interaction of a cellular 50 kDa protein with an RNA hairpin in the 5′ noncoding region of the poliovirus genome: evidence for a transient covalent RNA-protein bond. Proc. Natl. Acad. Sci. USA **87**:5846–5850.
24. **Nakhasi, H. L., X.-Q. Cao, T. A. Rouault, and T.-Y. Liu.** 1991. Specific binding of host cell proteins to the 3′-terminal stem-loop structure of rubella virus negative-strand RNA. J. Virol. **65**:5961–5967.
25. **Nakhasi, H. L., B. Meyer, and T.-Y. Liu.** 1986. Rubella virus cDNA: sequence and expression of E1 envelope protein. J. Biol. Chem. **261**:16616–16621.
26. **Nakhasi, H. L., T. A. Rouault, D. J. Haile, T.-Y. Liu, and R. D. Klausner.** 1990. Specific high-affinity binding of host proteins to the 3′ region of rubella virus RNA. New Biol. **2**:255–264.
27. **Nakhasi, H. L., N. K. Singh, G. P. Pogue, X.-Q. Cao, and T. R. Rouault.** Identification and characterization of host factor interactions with *cis*-acting elements of rubella virus RNA. *In* M. A. Brinton and R. Rueckert (ed.), Proceedings of the 3rd International Positive Strand RNA Virus Conference, in press. American Society of Microbiology. Washington, D.C.
28. **Nicholson, R., J. Pelletier, S.-Y. Le, and N. Sonenberg.** 1991. Structural and functional analysis of the ribosome landing pad of poliovirus type 2: in vivo translation studies. J. Virol. **65**:5886–5894.
29. **O'Brien, A. C., and J. B. Harley.** 1990. A subset of hy RNAs is associated with erythrocyte Ro ribonucleoproteins. EMBO J. **9**:3683–3689.
30. **Oker-Blom, C., N. Kalkkinen, L. Kääniänen, R. F. Pettersson.** 1983. Rubella virus contains one capsid protein and three envelope glycoproteins, E1, E2a, E2b. J. Virol. **46**:964–973.
31. **Oker-Blom, C., I. Ulmanen, L. Kääniänen, and R. F. Pettersson.** 1984. Rubella virus 40S genome RNA specifies a 24S subgenomic mRNA that codes for a precursor to structural proteins. J. Virol. **49**:403–408.
32. **Pardigon, N., and J. H. Strauss.** 1992. Cellular proteins bind to the 3′ end of Sindbis virus minus-strand RNA. J. Virol. **66**:1007–1015.
33. **Pelletier, J., G. Kaplan, V. R. Racaniello, and N. Sonenberg.** 1988. Cap-independent translation of poliovirus mRNA is conferred by sequence elements within the 5′ noncoding region. Mol. Cell. Biol. **8**:1103–1112.
34. **Pelletier, J., and N. Sonnenberg.** 1988. Internal initiation of translation of eukaryotic mRNA directed by a sequence derived from poliovirus RNA. Nature (London) **334**:320–325.
35. **Pogue, G. P., and T. C. Hall.** 1992. The requirement for a 5′ stem-loop structure in brome mosaic virus replication supports a new model for viral positive-strand RNA initiation. J. Virol. **66**:674–684.
36. **Pogue, G. P., N. K. Singh, X.-Q. Cao, and H. L. Nakhasi.** Unpublished data.
37. **Rader, M. D., C. O'Brien, Y. Liu, J. B. Harley, and M. Reichlin.** 1989. Heterogeneity of the Ro/SSA antigen. J. Clin. Invest. **83**:1293–1298.
38. **Rokeach, L. A., J. A. Haselby, J. F. Meilof, R. J. T. Smeenk, T. R. Unnasch, B. M. Greene, and S. O. Hoch.** 1991. Characterization of the autoantigen calreticulin. J. Immunol. **147**:3031–3039.
39. **Simoes, E. A. F., and P. Sarnow.** 1991. An RNA hairpin at the extreme 5′ end of the poliovirus RNA genome modulates viral translation in human cells. J. Virol. **65**:913–921.
40. **Wolin, S. L., and J. A. Steitz.** 1984. The Ro small cytoplasmic ribonucleoproteins: identification of the antigenic protein and its binding site on the Ro RNAs. Proc. Natl. Acad. Sci. USA **81**:1996–2000.
41. **Zheng, D., L. Dickens, T.-Y. Liu, and H. L. Nakhasi.** 1989. Nucleotide sequence of the 24S subgenomic mRNA of a vaccine strain (HPV77) of rubella virus: comparison with a wild type strain (M33). Gene **82**:343–349.